Accepted Manuscript

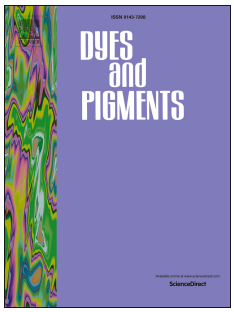

Novel hydro- and lipo-philic selenium zinc(II) phthalocyanines: Synthesis, photophysical properties and photodynamic effects on CT26 colon carcinoma cells

Sergio D. Ezquerra Riega, Nicolás Chiarante, Federico Valli, Julieta Marino, Leonor P. Roguin, Josefina Awruch, María C. García Vior

PII: S0143-7208(18)30082-2

DOI: 10.1016/j.dyepig.2018.03.067

Reference: DYPI 6652

To appear in: *Dyes and Pigments*

Received Date: 11 January 2018

Revised Date: 28 March 2018

Accepted Date: 28 March 2018

Please cite this article as: Ezquerra Riega SD, Chiarante Nicolá, Valli F, Marino J, Roguin LP, Awruch J, García Vior MaríC, Novel hydro- and lipo-philic selenium zinc(II) phthalocyanines: Synthesis, photophysical properties and photodynamic effects on CT26 colon carcinoma cells, *Dyes and Pigments* (2018), doi: 10.1016/j.dyepig.2018.03.067.

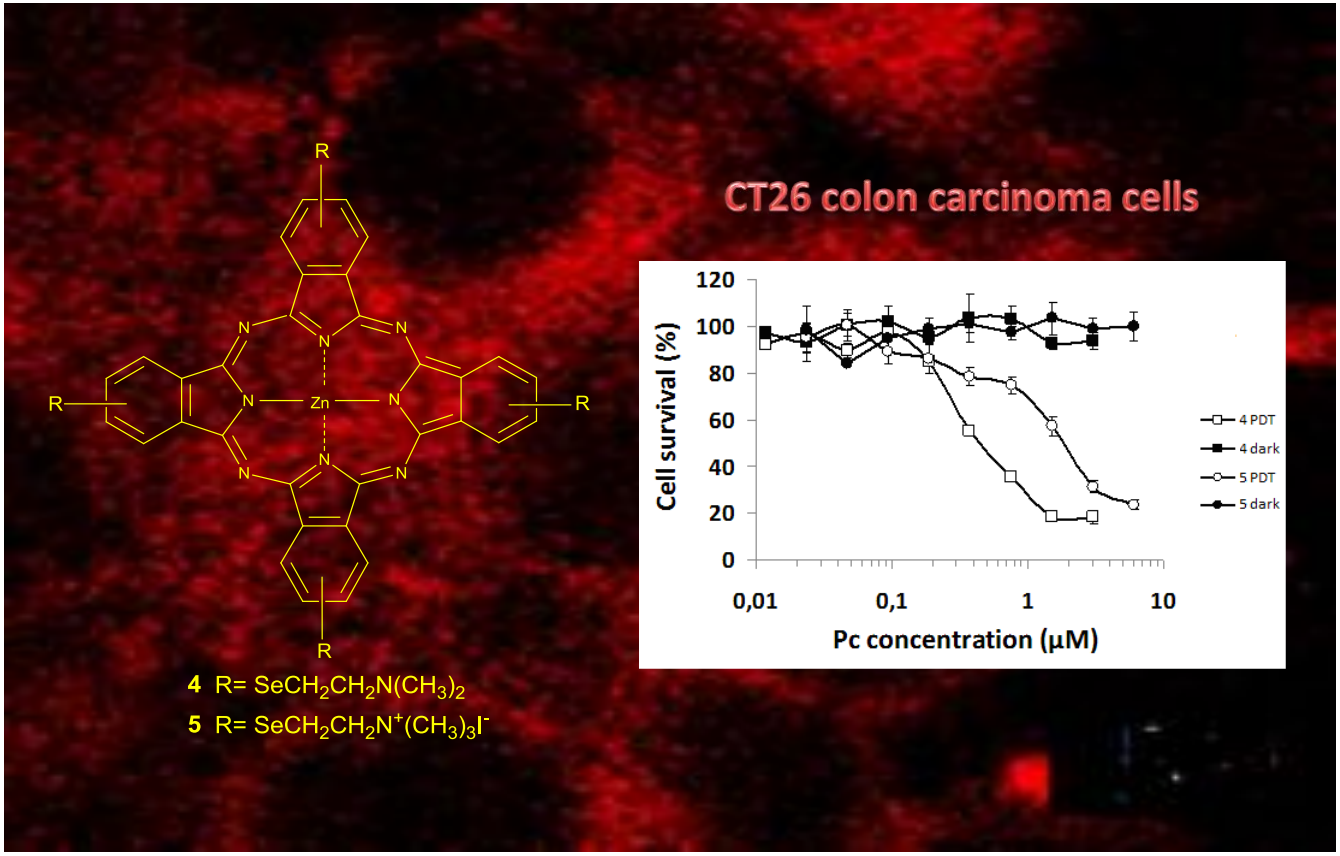
R
N
N
N
N
Zn
N
N
N
N
R
R
R
4 R= SeCH2CH2N(CH3)2
5 R= SeCH2CH2N+(CH3)3I-
CT26 colon carcinoma cells
Cell survival (%)
120
100
80
60
40
20
0
0,01
0,1
1
10
Pc concentration (μM)
4 PDT
4 dark
5 PDT
5 dark

Novel hydro- and lipo-philic selenium zinc(II) phthalocyanines: Synthesis, photophysical properties and photodynamic effects on CT26 colon carcinoma cells

Sergio D. Ezquerra Riega[a], Nicolás Chiarante[b], Federico Valli[b], Julieta Marino[b], Leonor P. Roguin[b], Josefina Awruch[a], María C. García Vior[a*]

[a] Universidad de Buenos Aires, Consejo Nacional de Investigaciones Científicas y Técnicas, Facultad de Farmacia y Bioquímica, Departamento de Química Orgánica, Junín 956, C1113AAD Buenos Aires, Argentina.
[b] Universidad de Buenos Aires, Consejo Nacional de Investigaciones Científicas y Técnicas, Instituto de Química y Fisicoquímica Biológicas (IQUIFIB), Facultad de Farmacia y Bioquímica, Junín 956, C1113AAD Buenos Aires, Argentina.

*Corresponding author. Tel. +54 11 528774305.
E-mail addresses: ceciliavior@gmail.com (M.C. García Vior)

In loving memory of Prof. Dr. Josefina Awruch

Abstract

The synthesis and photochemical properties of two novel selenium zinc(II) phthalocyanines, a lipid-soluble 2,9(10),16(17),23(24)-tetrakis[(2-dimethylamino)ethylselanyl]phthalocyaninato zinc(II) (**4**) and its water-soluble quaternized derivative 2,9(10),16(17),23(24)-tetrakis[(2-trimethylammonium)ethylselanyl]phthalocyaninato zinc(II) tetraiodide (**5**), were investigated. Maximum absorption values were 689 nm and 684 nm for 4 and 5 in DMF, respectively. In addition, phthalocyanines were revealed to be very efficient singlet oxygen generators with high values of Φ_Δ 0.74 and 0.84 for **4** and **5** in DMF, and they were photostable over the irradiation times studied. The photodynamic effect were evaluated on CT26 colon carcinoma cells. After light exposure, **4** and **5** were found to be cytotoxic, and IC_{50} values were 0.5 ± 0.1 μM and 2.3 ± 0.6 μM, respectively. The production of a greater amount of reactive oxygen species after phthalocyanines irradiation would be responsible for its potent phototoxic action on CT26 colon carcinoma cells.

Keywords: Photodynamic therapy, selenium zinc(II) phthalocyanines, Singlet oxygen, CT26 cells

1. Introduction

Colorectal carcinoma is one of the most common cancers and one of the leading causes of cancer-related death in the World. Conventional cancer treatments, such as chemotherapy, radiotherapy and surgery are aggressive therapies and produce significant systemic toxicity that causes severe short- or long-term side effects. Therefore, the use of alternative selective and noninvasive therapies that minimize systemic side effects are needed. In this context, photodynamic therapy (PDT) is a promising clinical treatment of a variety of endoscopically accessible tumors such as lung, bladder, gastrointestinal, and gynecological neoplasm, as well as non-melanoma skin cancer and precancerous diseases [1-7]. Phthalocyanines (Pc) are among the most promising second-generation photosensitizers as phototoxic drugs for PDT because they have high efficiency of reactive oxygen species generation upon illumination, high chemical stability and fluorescence [8-11]. Also, they have some advantages over hematoporphyrin derivatives, such as an absorption peak at a longer wavelength in the red light region, where tissue penetration is enhanced, a higher extinction coefficient at around two orders of magnitude stronger than the highest Q-band absorption of a porphyrin, and reduced skin phototoxicity. The photophysical properties of Pc are strongly influenced by the presence and nature of the coordinated central metal ion [12,13]. Zinc (II) phthalocyanines have intensive red-visible region absorption, high singlet and triplet yields and long lifetimes of the excited triplet, making them extremely valuable for PDT.

In PDT applications, an important issue related to Pc derivatives is their water solubility and aggregation properties, which may have a noticeable influence on the singlet oxygen production efficiency, bioavailability and the in vivo distribution of Pc. While lipophilic Pc are reported to have a higher tumor affinity, but associated with a higher cutaneous phototoxicity [14], cationic

Pc are considered the best targets for a new photosensitizers because they are able to improve water solubility and prevent the aggregation that seriously compromises the PDT value of the photosensitizer [15].

Bioisosterism represents in medicinal chemistry a successful strategy in the molecular modification and design of new therapeutically drugs [16]. Our group have previously reported the synthesis and photobiological studies of four isosteric water-soluble cationic zinc (II) phthalocyanines by using human nasopharynx KB carcinoma cells [17]. The sulfur-linked cationic dye, 2,9(10),16(17),23(24)-tetrakis[(2-trimethylammonium)ethylsulfanyl]phthalocyaninato zinc(II) tetraioidide (Pc13) was the most active of the four sensitizer assays and showed a singlet oxygen quantum yield (Φ_Δ) of 0.58 in water and a higher bathochromic shift of 10 nm for the Q-band as compared with the oxygen-linked cationic aliphatic phthalocyanine 2,9(10),16(17),23(24)-tetrakis[(2-trimethylammonium)ethoxy]phthalocyaninato zinc(II) tetra iodide. Moreover, no effect on cell proliferation was observed after light exposure of KB cells previously incubated with the oxygen isoster. The cytotoxic potency of the lipophilic phthalocyanine 2,9(10),16(17),23(24)-tetrakis-[(2-dimethylamino)ethylsulfanyl]phthalocyaninato zinc(II)) (Pc9) incorporated into poloxamine polymeric micelles was also studied in KB and murine colon adenocarcinoma cells (CT26 cells) demonstrating a remarkable more efficient capacity to reduce cell viability after photodynamic treatment than Pc13 [18, 19]. According to these observations, the bioisosteric replacement of the heteroatom attached to the phthalocyanine macrocycle should be studied since it can cause significant modifications in the photophysical and photodynamic properties that could be useful for the PDT requirements. We have reported the first synthesis of a lipophilic alkylselenium tetrasubstituted zinc(II) phthalocyanine which presented a Φ_Δ of 0.64, a fluorescence quantum yield (Φ_F) production of 0.18 and a high Q band absorption coefficient which is relevant for dosing in PDT studies [20].

These results have encourage us to investigate the synthesis, photochemical properties, photochemical stability and photobiological activity on murine colon carcinoma cells (CT26) of the selenium-linked lipophilic dye 2,9(10),16(17),23(24)-tetrakis[(2-dimethylamino)ethylselanyl]phthalocyaninato zinc(II) (**4**) and its water-soluble quaternized dye 2,9(10),16(17),23(24)-tetrakis[(2-trimethylammonium)ethylselanyl]phthalocyaninato zinc(II) tetraiodide (**5**).

2. Experimental

2.1 Materials

Chromatography columns were prepared with tlc Kiesegel (Merck), and Aluminium Oxide 90 standardized (Merck). *N*,*N*-dimethylformamide (DMF) was dried over 3Å molecular sieves during 72 hours, then filtered and freshly distilled before utilization [21]. Sodium hydride Riedel-de Haën 80% suspension in oil was employed. 1,3-Diphenylisobenzofuran (DPBF), tetrahydrofuran (THF) and 1,8-Diazabicyclo[5.4.0]undec-7-ene (DBU), as well as all reagents were provided by Sigma-Aldrich. Pc9 and Pc 13 were synthesized in our laboratory [19]. The probe 2',7'-dichlorfluorescein diacetate (DCFH-DA) and propidium iodide were obtained from Sigma Chemical.

2.2. Instrumentation

Melting points were determined on an Electrothermal 9100 capillary melting point apparatus. ^{1}H NMR were recorded on a Bruker MSL 300 spectrometer. The ^{1}H NMR of the phthalocyanines were recorded on a Bruker AM 600. Intermediates ESI-TOF mass spectroscopy was determined with a ZQ Micromass spectrometer. Phthalocyanines mass spectra were measured with a Bruker SolariX 12 T FT-ICRMS with nano-ESI. Ions were detected between m/z 400 and 2000, yielding a 2 Mword time-domain transient. Electronic absorption spectra were determined with a Shimadzu UV-3600 PC spectrophotometer. Fluorescence spectra were monitored with a

QuantaMaster Model QM-4 PTI spectrofluorometer. Infrared spectra were performed with a Perkin Elmer Spectrum One FT-IR spectrometer.

2.3. Synthesis

2.3.1. 4,4'-diselanediyldiphthalonitrile (**2**). A mixture of 4-aminophthalonitrile (**1**) (0.200 g, 1.4 mmol) and an aqueous HCl solution (2.7 mL, 5.4 mmol) was stirred at 0 ºC. A cold water solution of sodium nitrite (1 mL, 2 mmol) was added dropwise. Then, sodium acetate (0.440 g, 5.4 mmol) and acetate buffer (40 mL) were added at pH 4.5. KSeCN (0.288 g, 2 mmol) was added under vigorous agitation, and the solution was kept at 0 ºC for 3 h. The reaction mixture was extracted with CH_2Cl_2 (3 x 30 mL) and the combined extracts were washed with water (2 x 30 mL) and dried over Na_2SO_4. After evaporation in vacuo, the residue was dissolved in a small volume of CH_2Cl_2 and filtered through a silica-gel column packed and pre-washed with the same solvent. Two bands were eluted and evaporated in vacuo. The residue was recrystallized from ethanol. Yield: 0.215 g (75%); mp 184–186 ºC. IR (KBr, cm-1): 3466, 3435, 2233, 1638, 1266, 1108, 741, 706, 524. ^{1}H NMR (300 MHz, $CDCl_3$): δ 7.80 (m, 3H), 8.01 (m, 3H). MS (ESI): m/z (%) = $[M+Na]^+$ calcd for $C_{16}H_6N_4Se_2Na$: 436.88179; found: $[M+Na]^+$ 436.88119.

2.3.2. 4-((2-(dimethylamino)ethyl)selanyl)phthalonitrile. (**3**)

A mixture of 4,4'-diselanediyldiphthalonitrile (0.197 g, 0.487 mmol), 2-chloro-*N*,*N*-dimethylethanamine hydrochloride (0.246 g, 1.7 mmol) [22] and NaH (0.200 g, 8.3 mmol) in DMF (5 mL) was stirred under an Ar atmosphere at 60°C for 3 h. The reaction mixture was poured into water (30 mL) and extracted with CH_2Cl_2 (3 x 20 mL) and the organic phase was washed with water (3 x 30 mL) and dried over anhydrous Na_2SO_4. After evaporation in vacuo, the residue was dissolved in a small volume of CH_2Cl_2 and filtered through a silica-gel column packed and pre-washed with the same solvent. After evaporation of the solvent, the residue was

recrystallized from ethanol. Yield: 0.136 g (55 %); mp 115-116°C. IR (KBr, cm-1): 523, 670, 821, 1040, 1063, 1124, 1210, 1293, 1373, 1477, 1542, 1580, 2228, 2780, 2822, 2860, 2940, 2970, 3016. ^{1}H NMR (300 MHz, $CDCl_3$): δ 2.25 (s, 6 H), 2.67 (t, 2 H, J = 6), 3.14 (t , 2 H, J = 6), 7.56 (d, 1 H, J = 9), 7.66 (dd, 1 H, J = 3; 9), 7.73 (d, 1 H, J = 3). MS (ESI): m/z (%) = $[M+Na]^+$ calcd for $C_{12}H_{13}N_3NaSe$: 302.01672; found: $[M+Na]^+$ 302.01694. Anal. Calcd. for $C_{12}H_{13}N_3Se$: C, 51.81; H, 4.71; N,15.1. Found: C, 51.59; H, 4.73; N,15.01

2.3.3. 2,9(10),16(17),23(24)-tetrakis[(2-dimethylamino)ethylselanyl]phthalocyaninato zinc(II) (**4**).

A mixture of 3 (0.130 g, 0.468 mmol), anhydrous zinc acetate (0.160 g, 0.704 mmol), and 1,8 diazabicyclo[5.4.0]undec-7-ene (DBU) (0.2 mL,1.34 mmol) in anhydrous butanol was stirred and heated at 150 °C under Ar atmosphere for an hour. The mixture was cooled down and evaporated in vacuo. The green solid residue was dissolved in a small volume of CH_2Cl_2–CH_3OH (98:2) and filtered through an aluminum oxide column packed and pre-washed with the same solvent. After evaporation in vacuo, the dye was recrystallized from CH_2Cl_2–hexane. Yield 0.085 g (65%). IR (KBr, cm-1): 596, 743, 824, 901, 1032, 1095, 1193, 1263, 1405, 2767, 2814, 2851, 2970. ^{1}H NMR (600MHz, $CDCl_3$): δ 1.62 (br s, 24H, CH_3), 2.43 (m, 8H, CH_2N), 3.51 (m, 8H, $SeCH_2$), 7.05-8.06 (m, 12H, Ar). MS (nano-ESI): m/z (%) = $[M+Na]^+$ calcd for $C_{48}H_{52}N_{12}NaSe_4Zn$: 1201.01841; found: $[M+Na]^+$. 1201.01847. Anal. Calcd. for $C_{48}H_{52}N_{12}Se_4Zn$: C, 48.93; H, 4.45; N,14.27. Found: C, 48.80; H, 4.43; N,14.18.

2.3.3. 2,9(10),16(17),23(24)- tetrakis [(2-trimethylammonium)ethylselanyl]phthalocyaninato zinc(II) tetraiodide (**5**)

3 (0.035 g, 0.029 mmol) was stirred in a solution of CH_3I (3 mL, 50 mmol) and freshly distilled CH2Cl2 for 24 hours at 60ºC. After cooling at room temperature, the obtained power was centrifuged and resuspended in CH_2Cl_2 (4 mL) and centrifuged again. Yield: 0.034 g (70%). IR

(KBr, cm-1): 605, 669, 824, 901, 1034, 1097, 1262, 1400, 2916, 2966. ^{1}H NMR (600MHz, $CDCl_3$ δ 2.51 (s, 24H, CH_3), 3.24 (m, 8H, CH_2N), 3.84 (m, 8H, $SeCH_2$), 7.04-8.11(m, 12H, Ar), MS (nano-ESI): m/z (%) = [M^+] calcd for $C_{52}H_{68}N_{12}Se_4I_4Zn$: 1750.78937; found: [$M^+$] 1750.79201. Anal. Calcd. for $C_{52}H_{68}N_{12}Se_4I_4Zn$: C, 35.69; H, 3.92; N,9.6. Found: C, 35.58; H, 3.90; N,9.55.

2.4. Photophysical and photochemical parameters

2.4.1. Spectroscopic studies

Absorption and emission spectra were recorded at different concentrations employing a 10 x 10 mm quartz cuvette. All experiments were performed at room temperature. The emission spectra of **4** and **5** were collected at an excitation wavelength of 610 nm (Q-band) and recorded between 630 and 800 nm.

2.4.2. Fluorescence quantum yields

Fluorescence quantum yields (Φ_F) were determined by comparison with those of Pc9 (Φ_F = 0.28 in THF) [17] as reference at λexc = 610 nm for **4** and **5**. Calculations were performed by equation 1.

$$\Phi_F^S = \Phi_F^R \frac{I^S\left(1-10^{-A^R}\right)}{I^R\left(1-10^{-A^S}\right)}\left(\frac{n^S}{n^R}\right)^2 \quad (1)$$

where R and S superscripts refer to the reference and the sample respectively; I is the integrated area under the emission spectrum; A is the absorbance of solutions at the excitation wavelength and $\left(n^S/n^R\right)^2$ stands for the refractive index correction.

2.4.3. Quantum yield of singlet oxygen production

Standard chemical monitor bleaching rates were used to calculate the quantum yield of singlet

oxygen generation rates [23]. For Φ_Δ studies, 1,3-diphenylisobenzofuran (DPBF) was used as a singlet oxygen chemical quencher. To avoid chain reactions induced by DPBF in the presence of singlet oxygen, the absorbance of DPBF was under 1.9 employing a 10 x 10 mm quartz cuvette. DPBF decay at 410 nm was monitored. Polychromatic irradiation was performed using a projector lamp (Philips 7748SEHJ, 24V-250W) and a cut-off filter at 610 nm (Schott, RG 610) and a water filter were used to prevent ultraviolet and infrared radiation. Samples **4**, **5** and Pc13 (Φ_Δ = 0.71 in DMF)

[17], were irradiated within the same wavelength interval λ_1 - λ_2 and Φ_Δ was calculated according to equation 2 [24].

$$\Phi_\Delta^S = \Phi_\Delta^R \frac{r^S}{r^R} \frac{\int_{\lambda_1}^{\lambda_2} I_o(\lambda)(1-10^{-A^R(\lambda)})d\lambda}{\int_{\lambda_1}^{\lambda_2} I_o(\lambda)(1-10^{-A^S(\lambda)})d\lambda} \quad (2)$$

where r is the singlet oxygen photogeneration rate and the superscripts S and R stand for the sample and reference respectively, A is the absorbance at the irradiation wavelength and Io(λ) is the incident spectral photon flow (mol s^{-1} nm^{-1}). When the irradiation wavelength range is narrow, the incident intensity varies smoothly with wavelength and the sample and reference have overlapping spectra Io may be approximated by a constant value which may be drawn out of the integrals and cancelled.

2.4.4. Photo-oxidative stability

The photostability of **4** and **5** was determined by the decay of the Q-band intensity after exposure to red light [25]. The fluence rate was adjusted to 20 $mWcm^{-2}$. Measurements were performed under air in THF. Photodegradation rate constants k were calculated by equation (3).

$$\ln \frac{A_0}{A_t} = k.t \quad (3)$$

where t, A_0, A_t are the irradiation time, absorbance at t=0, absorbance at different times, respectively.

2.5. Biological Studies

2.5.1. Cells and culture conditions

Murine colon carcinoma CT26 cells (ATCC CRL-2638) were maintained in a humidified atmosphere of 5% CO2 at 37 ºC in RPMI-1640 (Gibco BRL) containing 10% (v/v) fetal bovine serum (FBS, Gibco BRL), 2 mM L-glutamine, 50 U/mL penicillin and 50 mg/mL streptomycin.

2.5.2 Photodynamic treatment

CT26 cells were plated at a density of 2 x 104 cells/well in 96-well microplates and incubated overnight at 37 °C until 70-80% of confluence. Then, the culture medium was replaced by medium containing 4% FBS and different concentrations of phthalocyanine **4** or **5**. Stock solutions of 0.83 mM phthalocyanine **4** dissolved in dimethyl sulfoxide (DMSO) and 5 mM phthalocyanine **5** prepared in water were employed. 24 h later, compounds were removed and cells were exposed to a light dose of 2.8 J cm^{-2}, 1.17 mW cm^{-2}, with a 150 W halogen lamp equipped with a 10 mm water filter to attenuate IR radiation and maintain cells cool. In addition, a cut-off filter was used to bar wavelengths shorter than 630 nm, as described previously [17]. In parallel, non-irradiated cells were used to study dark cytotoxicity. 24 h following treatment, cell viability was determined by the MTT reduction assay. The absorbance (595 nm) was measured in a Biotrack II Microplate Reader (GE Healthcare, Piscataway, NY).

2.5.3. Determination of intracellular reactive oxygen species (ROS) production

The endogenous ROS content was evaluated from the oxidation of the probe 2',7' dichlorofluorescein diacetate. After diffusing into cells, DCFH-DA is first deacetylated by esterases and then is oxidized by hydrogen peroxide or peroxides to produce the fluorescent

2',7'-dichlorofluorescein (DCF). CT26 cells were plated at a density of 3 x 10^4 cells/well in 24 well microplates and incubated 48 h at 37ºC until 70-80% of confluence. Then, the culture medium was replaced by RPMI containing 4% FBS and different concentrations of **4** or **5**. After 24 h, cells were washed with PBS and incubated incubated with a 10 μM concentration of DCFH-DA for 30 min at 37 ºC. After removing the probe, cells were irradiated with a light dose of 2.8 J cm^{-2} in the presence of RPMI containing 10% FBS. Cells were next solubilized by treating with Triton X-100 (0.1% v/v) in PBS for 30 minutes, and the green fluorescence of DCF was detected in a PerkinElmer LS55 Fluorometer (PerkinElmer Ltd., Beaconsfield, UK) using 488 nm excitation and 530 nm emission wavelengths. After 10 min of incubation with a final concentration of 50 μM propidium iodide (PI), DNA content was estimated from the fluorescence intensity of DNA-PI complex at excitation and emission wavelengths of 538 and 590 nm, respectively. Results were expressed as the ratio between DCF and PI fluorescence.

2.5.4. Statistical analysis

The values are expressed as mean ± S.E.M. Statistical analysis of the data was performed by using the Student´s t-test or one way analysis of variance (ANOVA) followed by Dunnett post hoc test where appropiate. $p<0.05$ denotes a statistically significant difference.

3. Results and Discussion

3.1. Synthesis

Novel selenium tetrasubstituted zinc (II) phthalocyanines compounds were designed and synthesized as depicted in Scheme 1. The sequence begins with the reaction of the commercially available 4-aminophthalonitrile (1) with sodium nitrite solution followed by the addition of potassium selenocyanate to give compound **2**. Phthalonitriles **2** reacted with excess of sodium hydride in DMF and 2-chloro-*N*,*N*-dimethylethanamine hydrochloride giving 3 in 55% yield [22]. Briefly, phthalocyanine **4** was prepared by cyclotetramerization of phthalonitrile **3** by using DBU in butanol and zinc acetate at 150 ºC. This dye was purified by chromatography,

followed by recrystallization to attain 55% of the desired 2,9(10),16(17),23(24)-tetrakis[(2 dimethylamino)ethylselanyl]phthalocyaninato zinc(II). Phthalocyanine **4** was further *N*-methylated using an excess of iodomethane in CH_2Cl_2 to give the cationic phthalocyanine **5** in a high yield of 70%. According to these, compounds **4** and **5** can be synthesized by a standard synthetic protocol and are thus obtained as a mixture of regioisomers.

In general metallophthalocyanine complexes are insoluble in most organic solvents and water; however the introduction of substituents on the ring increases their solubility. Phthalocyanine **4** showed excellent solubility in THF, DMF and DMSO. Quaternized complex was fully soluble DMF, DMSO and water. The presence of isomers has the positive effect of disrupting crystalling order and thus enhancing solubility; however it is a disadvantage if a pure photosensitizer is required for clinical purposes.

Intermediates **2-3** and phthalocyanines were characterized by UV-vis, IR and ^{1}H NMR and nano-ESI FT-ICR mass spectroscopy has become the choice method for the analysis of selenium compounds. The analyses are consistent with the predicted structures as shown in the experimental section.

Scheme 1

3.2. Spectroscopic studies

Spectroscopic properties of selenium zinc (II) phthalocyanines **4** and **5** are summarized in Table 1. The UV–visible absorption spectra of **4** and **5** was recorded in DMF in the 300-800 nm range. As shown in Fig. 1, the electronic spectra of **4** and **5** is typical for non-aggregated metallated phthalocyanines. It is characterized by the appearance of an intense and narrow Q band at 684-689 nm associated with some less intense satellites at its blue flank, the appearance of a less intense but broad Soret band at 367-370 nm and transparency in the other spectral region [23,26]. Furthermore, no deviations from the Lambert-Beer law was observed, indicating that they are esentially free from aggregation at the concentration studied. Compared with

oxygen containing phthalocyanines previously reported [17,27,28], selenium phthalocyanines present a bathochromic shift of 7–11 nm for the Q-bands. In addition, the Q band absorption coefficient of the selenium phthalocyanine **4** was 2 times higher than the isosteric oxygen dye, 2,9(10),16(17),23(24)-tetrakis[(2-dimethylamino)ethoxy]phthalocyaninato zinc(II) [17], this property improving skin light and it is relevant for dosing in PDT studies. Any differences in the Q-band absorption coefficient was observed when selenium phthalocyanine **4** and **5** were compared with their sulfur analogs previously published by our group [17] .

Table 1

Figure 1

The fluorescence spectrum of selenium zinc (II) tetrasubstituted phthalocyanines in DMF are shown in Fig. 1. The shape of the spectra for all dyes is the same as others zinc(II) phthalocyanines indicating that fluorescence can be attributed only to the monomer [27, 28]. The fluorescence Q peaks are shifted ~1 nm to the red from the corresponding absorption maximum (Table 1). Relative fluorescence quantum yields (Φ_F) are similar for compounds **4** and **5**.

3.3. Quantum yield of singlet oxygen production

Table 1 shows singlet oxygen quantum yield Φ_Δ values for dyes **4** and **5** in DMF. Sample absorbances were kept as low as possible to prevent aggregation in order to obtain measurable values of quantum yield of singlet molecular oxygen. The singlet oxygen generation mechanism does not cause any remarkable change in the absorption intensity of phthalocyanines which exhibit their stability during this experiment. As indicated in Table 1, phthalocyanines **4** and **5** are excellent singlet oxygen generators with a high value of Φ_Δ , 0.84 and 0.74, respectively.

3.4. Photo-oxidative stability

The photostability of **4** and **5** was analyzed in DMF by measuring the decrease in the intensity of the Q-band over time irradiation with red light under air. The time decay of the absorbance maxima of the Q-band for both compounds obeyed first-order kinetics as shown in

Fig. 2.

Figure 2

The corresponding photodegradation constants k are listed in Table 1. As shown in Table 1, phthalocyanines showed low values of k, thus indicating that they are stable over thee irradiation time of our experiments. Moreover cationic phthalocyanine **5** presented the highest photostability. This finding is consistent with the fact that the oxidative reactions, mediated by singlet oxygen, have no appreciable contribution in the photo-oxidation of positively charged Pc. Moreover, increasing the electron-withdrawing character of substituents at periphery of macro-ring by positive charge substantially enhances the photostability of zinc phthalocyanines [29].

3.5. Photocytotoxicity studies

The cytotoxic effect of different concentrations of the lipophilic phthalocyanine **4** (dissolved in 0.4% DMSO) and the hydrophilic phthalocyanine **5** (dissolved in culture medium) was examined on CT26 cells. As shown in Fig. 3, no change in cell survival was observed when cells were incubated in the dark up to a 6 μM concentration of any compound. However, a concentration dependent cytotoxicity was evident upon exposure to a light dose of 2.8 J cm^{-2}, 1.17 mW cm^{-2}. The comparison of the IC_{50} values, obtained from dose-response curves, revealed that **4** showed a higher potency than **5** (Table 2). This is consistent with the conclusion that lipophilic photosensitizers are preferentially transported by lipoproteins, which are uptaken directly by tumor cells and favoring the cell killing efficacy in comparison with the hydrophilic one, as reported by Jori and co-workers [30-32].

In a previous work, we demonstrated that sulfur-linked cationic aliphatic phthalocyanines are more effective photosentitizers than oxygen-linked cationic isosteric compounds [17, 33]. We then reported the photodynamic potency of Pc9, the hydrophobic sulfur-linked phthalocyanine analog of **4** [18] that represents an intermediary compound in the synthesis of Pc13, the water soluble sulfur-linked cationic dye isoster of **5** [17]. When the cytotoxic properties of these

compounds were studied in the human nasopharynx KB carcinoma cell line, a greater effect was achieved with the hydrophobic phthalocyanine (dissolved in DMSO) with respect to the hydrophilic one. Thus, IC_{50} values of 0.12 ± 0.07 μM and 2.7 ± 0.6 μM were obtained for Pc9 and Pc13, respectively [17, 18]. In addition, the photodynamic activity of Pc9 significantly increased after its incorporation into different carriers, such as liposomes and micelles [18, 34]. For comparative purposes, in this work we decided to examine the phototoxic activity of these sulfur-linked phthalocyanines in CT26 cells. Under the same experimental conditions herein employed, a 50% cell growth inhibition was obtained at 0.7 ± 0.1 μM of Pc9 and 1.4 ± 0.3 μM of Pc13 (Table 2). After light exposure, the selenium isosters 4 and 5 were found to be cytotoxic, and IC50 values were 0.5 ± 0.1 μM and 2.3 ± 0.6 μM, respectively. These findings revealed that although lipophilic compounds exhibited higher potency than the water-soluble dyes, a similar antitumor action was obtained for selenium- and sulfur-linked phthalocyanines regardless of their hydrophobic properties.

3.6. Production of reactive oxygen species

An appropriate photosensitizer should induce the intracellular production of ROS, cytotoxic molecules responsible of the oxidative damage that may result in cell death [35,36]. In order to explore the ability of both selenium-linked phthalocyanines to generate ROS, Pc-loaded CT26 cells were incubated with DCFH-DA, a probe which is oxidized to a fluorescent compound in the presence of ROS. After irradiation of tumor cells, ROS formation was proportional to the photocytotoxicity of each phthalocyanine. Thus, a significant increment in ROS levels was detected at Pc concentrations representing the corresponding IC_{50} values, increasing ROS formation in a concentration-dependent manner (Fig. 4).

4. Conclusions

The syntheses, photochemical properties, photochemical stability and photobiological activity on murine colon carcinoma cells (CT26) of the selenium-linked lipophilic dye **4** and its water-

soluble quaternized dye **5** were investigated. Phthalocyanines were prepared by a one-step cyclotetramerization reaction of the corresponding phthalonitrile in the presence of $Zn(OAc)_2$ in good yields and consequently are mixtures of regioisomers. In addition, the phthalocyanines were revealed to be very efficient singlet oxygen generators with a high value of Φ_Δ 0.74 and 0.84 for **4** and **5** in DMF, respectively and exhibited remarkable photostability over the irradiation times studied. Phthalocyanines **4** and **5** had no dark toxicity and showed an effective photodynamic activity in CT26 cells. A higher cytotoxic effect was obtained with the lipophilic phthalocyanine **4** (IC_{50}= 0.5 ± 0.1 μM) with respect to the hydrophilic phthalocyanine **5** (IC_{50}= 2.3 ± 0.6 μM). In accordance with this result, lower concentrations of **4** were required to generate ROS and induce a more potent cell death. These results showed that the synthesized phthalocyanines are promising candidates for PDT application and encourage us to carry out further in vivo studies after the investigation of pure isomers isolation.

Acknowledgments

This work was supported by grants from the University of Buenos Aires, (Programación científica 2014-2017, UBACyT 20020130100024), the Consejo Nacional de Investigaciones Científicas y Técnicas (CONICET, PIP 066) and the Agencia Nacional de Promoción Científica y Tecnológica (PICT 2013-1844) Buenos Aires, Argentina. We wish to thank the technical assistance as regards chromatography of Ms. Juana Alcira Valdez and Lucia Mercedes Luquez and the mass spectroscopy assistance of Diego Cobice.

References

[1] Doughtery TJ, Gomer CJ, Henderson BW et al. Photodynamic therapy. J. Natl. Cancer Inst. 1998:90: 889-905.

[2] Detty MR, Gibson SL, Wagner SJ. Current clinical and preclinical photosensitizers for use in photodynamic therapy. J. Med. Chem. 2004:47:3897-915.

[3] Simone CB, Friedberg JS, Glatstein E, Stevenson JP, Sterman DH, Hahn SM, Cengel KA. Photodynamic therapy for the treatment of non-small cell lung cancer. J Thorac Dis. 2012:4:63-75.

[4] Photodynamic therapy of bladder cancer. A new option. Neuhaus J, Schastak S, Berndt M, Walther J, Dietel A, Sieger N, Stolzenburg JU. Urologe A. 2013:52:1225-32.

[5] Chen JJ, Gao LJ, Liu TJ. Photodynamic therapy with a novel porphyrin-based photosensitizer against human gastric cancer. Oncology Lett. 2015:11:775-81

[6] Koren H, Alth G. Photodynamic therapy in gynaecologic cancer. J. Photochem. Photobiol. B. 1996:35:189-91.

[7] Cohen D, Lee PK. Photodynamic Therapy for Non-Melanoma Skin Cancers. Cancers. 2016:8:90-9.

[8] Ali H, van Lier JE. Metal complexes as photo- and radiosensitizers. Chem Rev 1999;99:2379-2450.

[9] MacDonald IJ, Dougherty TJ. Basic Principles of photodynamic therapy. J Porphyrins Phthalocyanines 2001;5 :105-29.

[10] Detty MR, Gibson SL, Wagner SJ. Current Clinical and Preclinical Photosensitizers for Use in Photodynamic Therapy. J Med Chem 2004;47:3897-915.

[11] Moeno S, Krause RWM, Ermilov EA, Kuzyniak W, Höpfner M. Synthesis and characterization of novel zinc phthalocyanines as potential photosensitizers for photodynamic therapy of cancers. Photochem Photobiol Sci 2014;13: 963-70.

[12] Bonnett R. Photosensitizers of the porphyrin and phthalocyanine series for photodynamic therapy. Chemical Society Reviews 1995;24:19-33.

[13] Tedesco AC, Rotta JCG, Lunardi CN. Synthesis, photophysical and photochemical aspects of phthalocyanines for photodynamic therapy. Current Organic Chemistry 2003;7:187-96.

[14] Jori, G. J. Tumour photosensitizers: Approaches to enhance the selectivity and efficiency of photodynamic therapy. Photochem. Photobiol. B: Biol. 1996;36,87-93.

[15] Durmus M¸ Yaman H, Göl C, Ahsen V, Nyokong T. Water-soluble quaternized mercaptopyridine-substituted and bovine serum albumin binding properties. Dyes and Pigments 2011;91:153-63.

[16] Moreira Lima L, Barreiro EJ. Bioisosterism: A Useful Strategy for Molecular Modification and Drug Design. Curr Med Chem. 2005;12:23-49.

[17] Marino J, García Vior MC, Dicelio LE, Roguin LP, Awruch J. Photodynamic effects of isosteric water-soluble phthalocyanines on human nasopharynx KB carcinoma cells. Eur. J. Med. Chem. 2010;45: 4129-39.

[18] Chiarante N, García Vior MC, Awruch J, Marino J, Roguin LP. Phototoxic action of a zinc(II) phthalocyanine encapsulated into poloxamine polymeric micelles in 2D and 3D colon carcinoma cell cultures J. Photochem Photobiol. B: Biol. 2017;170:140–151.

[19] García Vior MC, Marino J, Roguin LP, Sosnik A, Awruch J. Photodynamic Effects of Zinc(II) Phthalocyanine-Loaded Polymeric Micelles in Human Nasopharynx KB Carcinoma Cells. Photochem Photobiol. 2013;89:492–500.

[20] Ezquerra Riega SD, García Vior MC, Awruch J. Synthesis and properties of a novel alkylselenium substituted phthalocyanine. Tetrahedron Lett. 2015;56:4047-49.

[21] Burfield DR, Smithers RH. Desiccant efficiency in solvent drying. Dipolar aprotic solvents.

J Org Chem 1978;43:3966-68.

[22] Hall LAR, Stephens VC, Burckhalter JH. β-dimethylaminoethyl chloride hidrochloride [Ethylamine, 2-chloro-*N*,*N*-dimethyl-, hydrochloride] Organic Syntheses Coll. 1963;4:333-8.

[23] Lagorio MG, Dicelio LE, San Román E. Visible and near IR spectroscopical and photochemical characterization of substituted metallophthalocyanines. J Photochem. Photobiol A: Chemistry 1993;72:153-61.

[24] Amore S, Lagorio MG, Dicelio LE, San Román E. Photophysical properties of supported dyes. Quantum yield calculations in scattering media. Prog. React. Kinet. Mech. 2001;26:159-77.

[25] Schnurpfeil G, Sobbi AK, SpillgerW, Kliesch H,Wöhrle DJ. Photo-oxidative stability and its correlation with semi-empirical MO calculations of various tetraazaporphyrin derivatives in solution. J Porphyrins Phthalocyanines 1997;1:159–67.

[26] Stillman MJ, Nyokong T. In: Leznoff CC, Lever ABP, editors. Phthalocyanines: properties and applications, Vol. 1. New York: VCH Publishers; 1989 [Chapter 3].

[27] Strassert CA, Dicelio LE, Awruch J. Reduction of an Amido Zinc(II) Phthalocyanine by Diborane. Synthesis 2006;799–802.

[28] Ogunsipe A, Maree D, Nyokong T. Solvent effects on the photochemical and fluorescence properties of zinc phthalocyanine derivatives. Journal of Molecular Structure 2003;650: 131–40.

[29] Kuznetsova NN, Kaliya OL. Oxidative photobleaching of phthalocyanines in solution. Porphyrins Phthalocyanines 2012;16:709–712.

[30] Jori G, In vivo transport and pharmacokinetic behavior of tumour photosensitizers. Ciba Found Symp. 1989;146:78–86.

[31] Valduga G, Giartluca Biartco I, Csik G, Red E, Masiero L, Garbisa S, Jori G. Interaction of Hydro- or Lipophilic Phthalocyanines with Cells of Different Metastatic Potential. Biochemical Pharmacology 1996;51:585-90.

[32] Decreau R, Richard M-J, Julliard M. Photodynamic therapy against achromic M6 melanocytes: phototoxicity of lipophilic axially substituted aluminum phthalocyanines and hexadecahalogenated zinc phthalocyanines. J. Porphyrins Phthalocyanines 2001; 5: 390–6.

[33] Gauna GA, Marino J, García Vior MC, Roguin LP, Awruch. Synthesis and comparative photodynamic properties of two isosteric alkyl substituted zinc(II) phthalocyanines. Eur. J. Med. Chem. 2011;46:5532-9.

[34] López Zeballos NC, Marino J, García Vior MC, Chiarante N, Roguin LP, Awruch J, Dicelio LE. Photophysics and photobiology of novel liposomal formulations of 2,9(10),16(17),23(24)-tetrakis[(2-dimethylamino)ethylsulfanyl]phthalocyaninatozinc(II). Dyes and Pigments 2013;96: 626-35.

[35] Sharman WM, Allen CM, van Lier JE. Photodynamic therapeutics: basic principles and clinical applications, Drug Discov. Today 1999;4:507-17.

[36] Agostinis P, Berg K, Cengel KA, Foster TH, Girotti AW, Gollnick SO, Hahn SM, Hamblin MR, Juzeniene A, Kessel D, Korbelik M, Moan J, Mroz P, Nowis D, Piette J, Wilson BC, Golab J. Photodynamic therapy of cancer: an update. CA Cancer J Clin. 2011;61:250-81.

Figure legends

Scheme 1. Synthetic route of phthalocyanines 4 and 5. Reagents and conditions: (a) HCl 2M $NaNO_2$ 2M, 0ºC; buffer acetate; KSeCN; 0ºC; 3h, 75%; (b) 2-chloro-*N*,*N*-dimethylethanamine hydrochloride; NaH, DMF, 60ºC, 3h, 55%; (c) $Zn(AcO)_2$, DBU, BuOH, reflux, 1h, 65%; (d) CH_3I, CH_2Cl_2, reflux, 24h, 70%.

Table 1. Photophysical parameters and photodegradation constants *k* obtained for **4** and **5** in DMF.

Fig. 1. Absorption and fluorescence spectra of phthalocyanine **4** and **5** in DMF.

Fig. 2. First-order plots for the photodegradation of phthalocyanine **4** and **5** in DMF.

Fig. 3. Effect of **4** and **5** on CT26 cell viability. Different concentrations of Pc were incubated with CT26 cells in the dark (**4** ■; **5** ●) or exposed to a light dose of 2.8 J cm^{-2} (**4** □; **5** ○). After 24 h of incubation, cytotoxicity was assessed by the MTT assay, as described under Experimental. Results are expressed as the percentage of cell survival obtained in the absence of phthalocyanine and represent the mean ± S.E.M. of three different experiments.

Table 2. Photocytoxicity of selenium phthalocyanines **4** , **5** and the sulfur isosteric analogs Pc9 and Pc13 in CT26 colon carcinoma cell lines.

Fig. 4. Intracellular ROS production after irradiation of Pc-loaded CT26 cells. Cells incubated for 24 h in the presence or absence (grey bar) of different concentrations of **4** (white bars) and **5** (black bars), were treated with a 10 μM concentration of DCFH-DA for 30 min at 37 ºC. After removing the probe, cells were irradiated and solubilized as indicated in Materials and methods. DCF fluorescence was measured in a fluorometer and DNA content was estimated after staining with a final concentration of 50 μM PI in the dark. Results are expressed as the ratio between DCF and PI fluorescence, and represent the mean ± S.E.M. of three different experiments. Statistical significance in comparison with the corresponding control values is indicated by *p< 0.005.

Compound	Solvent	λ_{max},Q-band (nm)	λ_{max}, Emission (nm)*	ε_{max} ($M^{-1}cm^{-1}$)	Φ_F	Φ_Δ	k ($10^{-3}min^{-1}$)
4	DMF	689	691	$(1.34 \pm 0.15)x10^5$	0.14 ± 0.01	0.85 ± 0.02	34
5	DMF	684	685	$(1.43 \pm 0.33)x10^5$	0.13 ± 0.01	0.74 ± 0.03	6

Table 1

Compound	IC_{50} (μM)[a]
4	0.5 ± 0.1
5	2.3 ± 0.6
Pc **9**	0.7 ± 0.1
Pc **13**	1.4 ± 0.3

[a] The molar drug concentrations required to cause 50% growth inhibition (IC_{50}) were determined from dose-response curves. Results represent the mean ± S.E.M of at least three different experiments.

Table 2

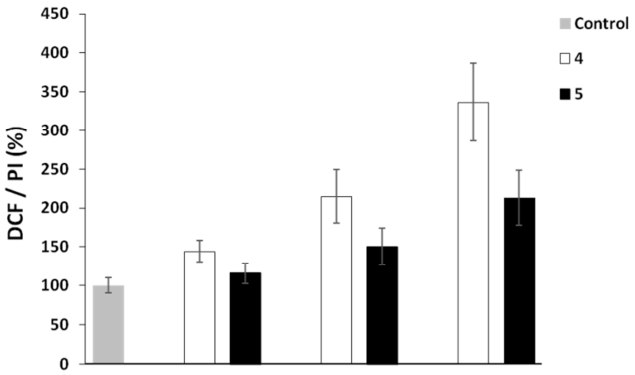

Figure 4

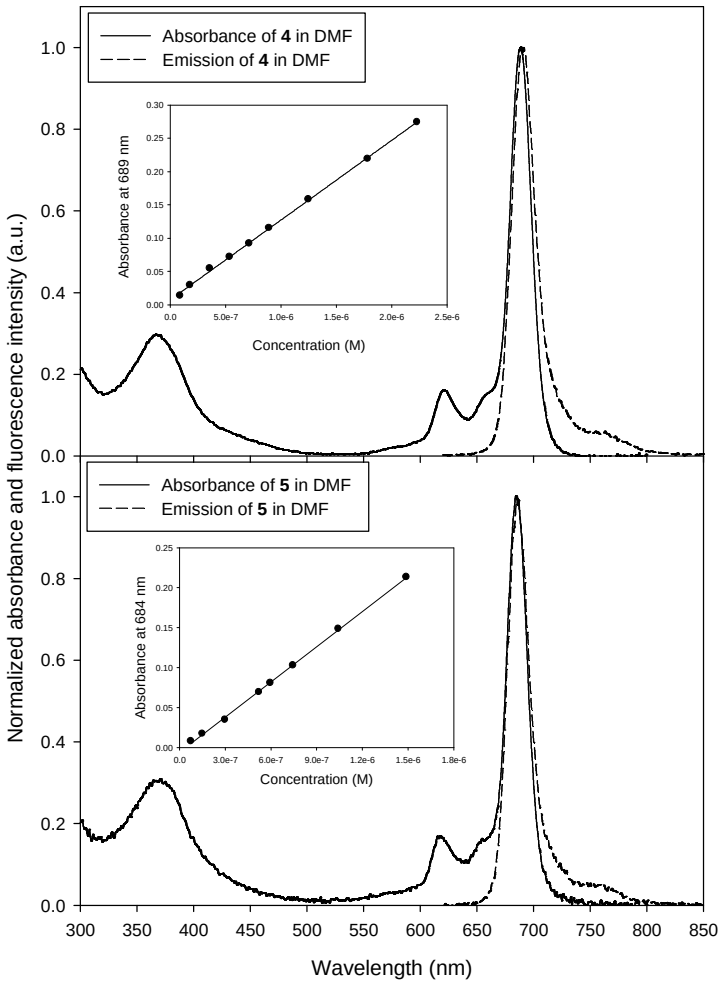

Figure 1

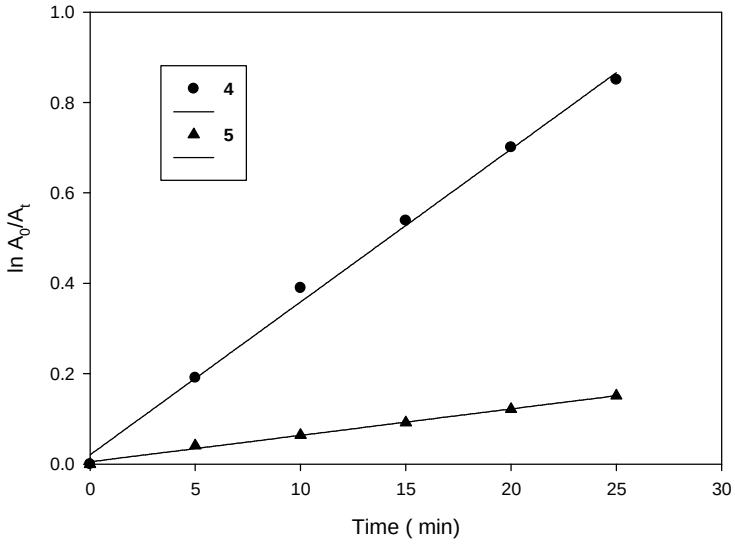

Figure 2

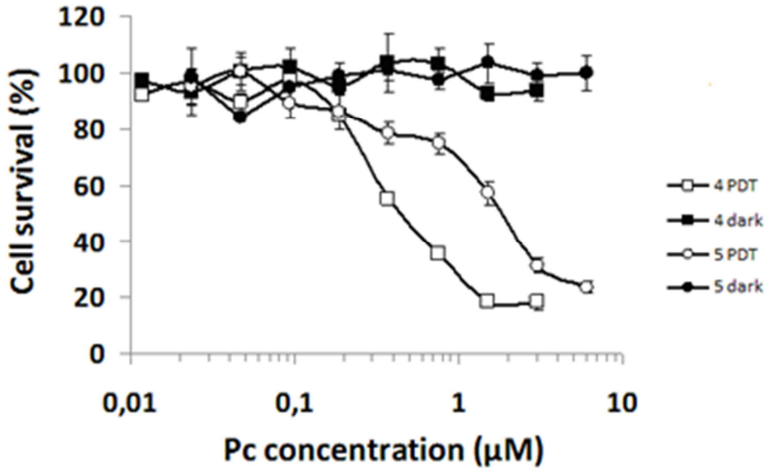

Figure 3

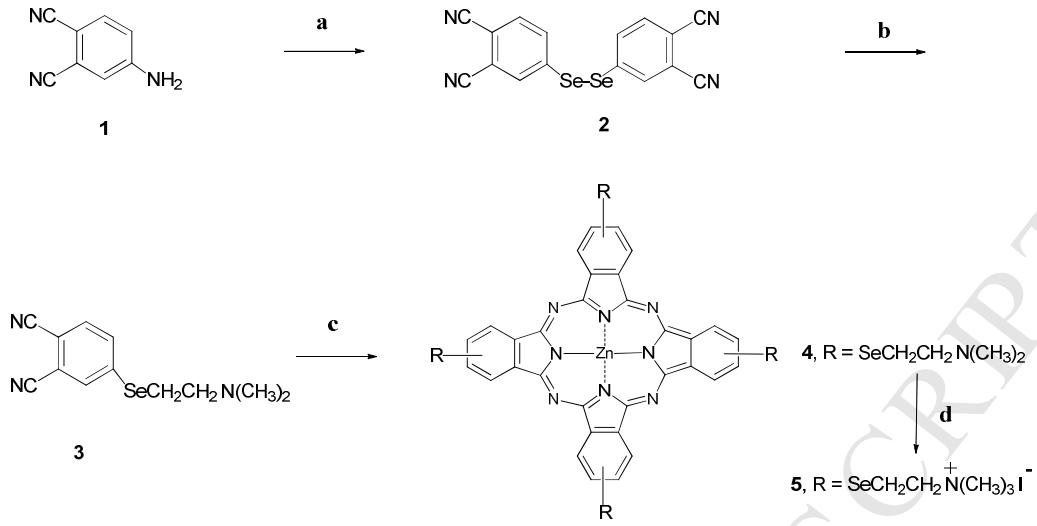

Scheme 1

Highlights

Novel hydro- and lipo-philic selenium zinc(II) phthalocyanines are synthetized.

The phthalocyanines are efficient singlet oxygen quantum yield generators.

The photodynamic effect is evaluated on murine colon carcinoma CT26 cells.

Lipophilic selenium phthalocyanine shows a higher phototoxicity (IC_{50}= 0.5±0.1 μM).

Water soluble selenium phthalocyanine presents the highest photostability.